

CrossMark  
click for updatesCite this: *CrystEngComm*, 2015, 17, 8807Received 3rd June 2015,  
Accepted 30th July 2015

DOI: 10.1039/c5ce01074h

www.rsc.org/crystengcomm

# Solvent-induced single-crystal to single-crystal transformation of a Zn<sub>4</sub>O-containing doubly interpenetrated metal–organic framework with a *pcu* net<sup>†</sup>

Jae Hwa Lee,<sup>a</sup> Tae Kyung Kim,<sup>a</sup> Myunghyun Paik Suh<sup>\*b</sup> and Hoi Ri Moon<sup>\*a</sup>

Guest molecules in a metal–organic framework (MOF), [Zn<sub>4</sub>O(CPMA)<sub>3</sub>]-6DMF (DMF = *N,N*-dimethylformamide), with an interpenetrating *pcu* net were exchanged with benzene, *n*-hexane, and methanol in a single-crystal to single-crystal (SC–SC) manner, which involved the sliding motion of the interpenetrating network, as well as the dynamic movements of the molecular components, and was triggered by host–guest interactions.

Metal–organic frameworks (MOFs), which respond to external stimuli such as guest removal/reintroduction, guest exchange, oxidation, pressure, temperature, and light, are potentially viable candidates for applications in sensing, separation, catalysis, and sorption.<sup>1</sup> The structural rearrangement of molecular components responding to a specific stimulus induces an immediate effect on the chemical or physical properties of MOFs.<sup>2</sup> Thus, direct observations of structural changes in MOFs using single-crystal X-ray diffraction (SCD) facilitate the understanding of their behaviours, and aid in the design of MOFs with superior performance. Over the past decade after Fujita's and Suh's groups reported the first single-crystal to single-crystal (SC–SC) transformation phenomenon for coordination polymers,<sup>3</sup> numerous examples of SC–SC transformations have been reported,<sup>4–10</sup> such as those on guest removal,<sup>5</sup> guest exchange,<sup>6</sup> temperature change,<sup>7</sup> ligand exchange,<sup>8</sup> metal ion exchange,<sup>9</sup> and addition of metal ions and anions.<sup>10</sup>

The guest-induced dynamic structural changes of MOFs are the important phenomena that can be applied to sensor

technologies. If the transformation occurs in a SC–SC manner upon guest exchange, it can provide meaningful and direct structural information about the property change such as the pore structure, luminescence, and magnetism. The SC–SC transformation occurs only in solvent exchange when the framework is robust yet flexible. In this context, interpenetrating MOFs can serve as appropriate systems, as several interesting observations regarding this have been reported.<sup>11–14</sup> For example, Kitagawa *et al.* reported an  $\alpha$ -polonium-type doubly interpenetrated 3D MOF,<sup>12</sup> which retained its single crystallinity during dehydration and rehydration with a concomitant colour change; moreover, the anion exchange between N(CN)<sub>2</sub><sup>−</sup> and N<sub>3</sub><sup>−</sup> induced slippage of the two independent networks and an increase in channel size. The same group developed a flexible doubly interpenetrated porous framework for a chemosensor by using its structural dynamics in response to the incorporation of

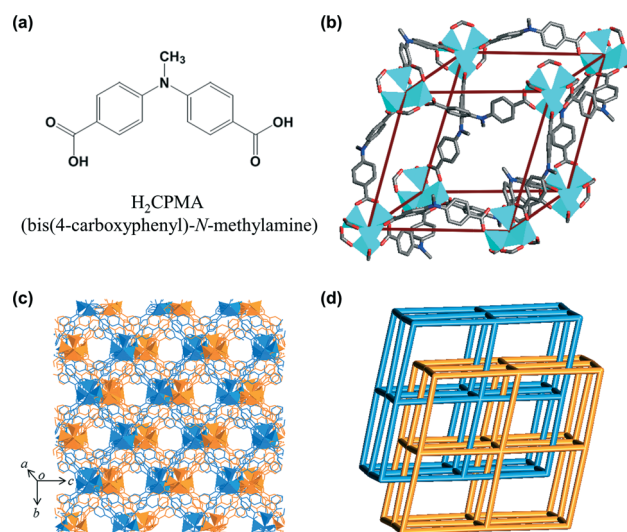


Fig. 1 (a) Organic ligand H<sub>2</sub>CPMA. (b) A single network unit with *pcu* topology composed of Zn<sub>4</sub>O clusters and CPMA<sup>2−</sup> ditopic ligands. (c–d) Doubly interpenetrated 3D framework and its simplified view.

<sup>a</sup> Department of Chemistry, Ulsan National Institute of Science and Technology (UNIST), 50 UNIST-gil, Ulsan 689-798, Republic of Korea.

E-mail: hoirimoon@unist.ac.kr

<sup>b</sup> Department of Chemistry, Hanyang University, Seoul 133-791, Republic of Korea. E-mail: mpsuh@snu.ac.kr

<sup>†</sup> Electronic supplementary information (ESI) available. CCDC 1403842–1403845 for compounds 1, 1<sub>benzene</sub>, 1<sub>hexane</sub>, and 1<sub>MeOH</sub>. Experimental details, IR spectra, TGA/DSC traces, photograph of single crystals, powder XRD patterns, and tables of X-ray crystallographic data for 1, 1<sub>hexane</sub>, 1<sub>MeOH</sub>, and 1<sub>benzene</sub>. X-ray crystallographic files in CIF format. For ESI and crystallographic data in CIF or other electronic format see DOI: 10.1039/c5ce01074h

chemically diverse analytes, which were proven by SCD studies.<sup>13</sup> Another interesting interpenetrating MOF showing SC–SC transformations was reported by Barbour's group.<sup>14</sup> The as-synthesized doubly interpenetrated MOF converted to its triply interpenetrated analogue upon desolvation, as monitored by SCD, and its conversion mechanism was proposed based on the computational results.

Previously, we published a paper regarding SC–SC transformations of a Li-based MOF upon immersion into explosive nitro compounds.<sup>15</sup> The results clearly revealed that the change in its fluorescence properties originated from the newly formed host–guest interactions. This interesting behaviour was attributed to the flexible ligand, bis(4-carboxyphenyl)-*N*-methylamine (H<sub>2</sub>CPMA), which simultaneously contains electron-donating and electron-withdrawing groups, and also has rotating sites on tertiary amine and carboxylate groups (Fig. 1a). Thus, in this study, we chose the same flexible CPMA ligand to build a new 3D doubly interpenetrated MOF, which was expected to exhibit dynamic structural changes upon guest exchange with organic solvents. In order to explore the types and strength of the interactions with the phenyl rings in CPMA<sup>2-</sup>, benzene, hexane and methanol were selected as exchanging solvents. Due to the SC–SC transformation upon guest exchange, the effects of the host–guest interactions on the motions of the molecular components in the coordination framework were directly observed.

The solvothermal reaction of Zn(NO<sub>3</sub>)<sub>2</sub>·6H<sub>2</sub>O and H<sub>2</sub>CPMA in DMF (DMF = *N,N*-dimethylformamide) resulted in the formation of deep-orange coloured crystals of [Zn<sub>4</sub>O(CPMA)<sub>3</sub>]·6DMF (**1**) based on the elemental analysis results. SCD analysis revealed that **1** crystallized in the trigonal space group *R*32 and had a *pcu* net topology composed of Zn<sub>4</sub>O clusters as octahedral secondary building units (SBUs) and CPMA<sup>2-</sup> ditopic ligands (Fig. 1b). The asymmetric unit of **1** contained two kinds of Zn<sub>4</sub>O clusters with one-third occupancy for each type of cluster, two CPMA<sup>2-</sup> ligands, as well as disordered solvent molecules. Even though the electron densities of some guest solvent molecules were observed, they could not be suitably modelled due to severe disorder. Thus, the SQUEEZE option of PLATON was used to remove the electron densities in the void.<sup>16</sup> The *pcu* net was distorted to a parallelepiped structure, due to the curved dicarboxylate ligand CPMA<sup>2-</sup> (Fig. 1b), and the framework was doubly interpenetrated to generate curved 3D channels (Fig. 1c and d). There were  $\pi$ – $\pi$  interactions between the phenyl rings of CPMA<sup>2-</sup> belonging to two interpenetrated nets (shortest C···C distances, 3.519–3.703 Å; dihedral angles, 58.88–83.37°) (Fig. S1†). PLATON calculations indicated that **1** contained 48.4% void space (103 333.5 Å<sup>3</sup> per unit cell volume), which was occupied by the guest molecules. As seen in the thermogravimetric analysis (TGA) trace of as-synthesized **1** (Fig. S2, ESI†), the guest solvent molecules were completely removed upon heating from room temperature to *ca.* 150 °C with an experimentally determined weight loss of 28.7%, which was in good agreement with the calculated weight loss of 28.8%. However, the

N<sub>2</sub>-sorption isotherm of dried **1** revealed no porosity because **1** showed flexibility, as evidenced by the X-ray powder diffraction (XRPD) patterns shown in Fig. S3†. Since dried MOF **1** lost transparency as well as single crystallinity, its SCD could not be obtained. However, the original structure of **1** was restored upon exposure to DMF vapour for 3 days at room temperature, indicating the reversibility of the structural movements.

As revealed by the guest removal and re-immersion experiments, **1** had a flexible structure, which was strongly influenced by the presence of guest molecules (Fig. S4–6†). In order to determine the effects of different types of guest molecules on the structural changes, guest-exchange experiments were conducted. When single crystal **1** was immersed in benzene, hexane, and methanol, in which **1** was insoluble, its crystallinity was retained, resulting in the formation of **1**<sub>benzene</sub>, **1**<sub>hexane</sub>, and **1**<sub>MeOH</sub>, respectively, which were suitable for SCD analysis. The exchange process was traced by Fourier transform nuclear magnetic resonance (FT-NMR) spectroscopy, and the results revealed that the exchange was terminated in three days (Fig. S7†). After solvent exchange, Fourier transform infrared (FT-IR) spectroscopy (Fig. S8†) revealed that the C=O stretching vibration of DMF molecules at 1661 cm<sup>-1</sup> in **1** clearly disappeared. Instead, new peaks corresponding to the exchanged guest molecules appeared at ~3090 cm<sup>-1</sup> for benzene ( $\nu_{\text{C-H(benzene)}}$ ), ~2990 cm<sup>-1</sup> for *n*-hexane ( $\nu_{\text{C-H(hexane)}}$ ), and ~3340 cm<sup>-1</sup> for methanol ( $\nu_{\text{O-H(methanol)}}$ ). During guest exchange, the possibility of dissolution and recrystallization of **1** in the new solvents was excluded based from photographs obtained with an optical microscope during immersion of the crystals, which also indicated the preservation of the single crystallinity of **1** during the exchange process (Fig. S9†).

SCD analysis revealed the dynamic movement of the interpenetrated nets (Fig. 2) upon guest exchange. In the structure of **1**, adjacent interpenetrated nets created two interesting spaces, which were composed of two phenyl rings from each net (Fig. 2a). In the A site, a pair of two phenyl rings had an edge-to-edge geometry with a dihedral angle of 64.07°, but in the B site, the phenyl rings were parallel to each other with a dihedral angle of 5.06°, creating a face-to-face geometry with an offset angle of 29.30°. These sites subsequently acted as important spaces for exchanged guest molecules to selectively fit into, depending on the preferred interactions. In **1**<sub>benzene</sub>, benzene molecules were located in A sites with edge-to-face  $\pi$ – $\pi$  interactions with the two phenyl rings of CPMA ligands (Fig. 2b) (shortest C···C distances, 3.883 Å; dihedral angles, 47.99°). Meanwhile, the dihedral angle between two phenyl rings of the framework showed minor changes (66.36°). This was sufficient for the guest molecules to form the strongest  $\pi$ – $\pi$  interactions without significant alteration of the host framework because edge-to-face  $\pi$ – $\pi$  interactions are more stable than face-to-face interactions.<sup>17</sup> In **1**<sub>hexane</sub>, the included *n*-hexane molecules formed CH– $\pi$  interactions with the two phenyl rings of the CPMA<sup>2-</sup> ligands in the B sites (shortest C···C distances, 3.919 and 4.016 Å) (Fig. 2c). The space

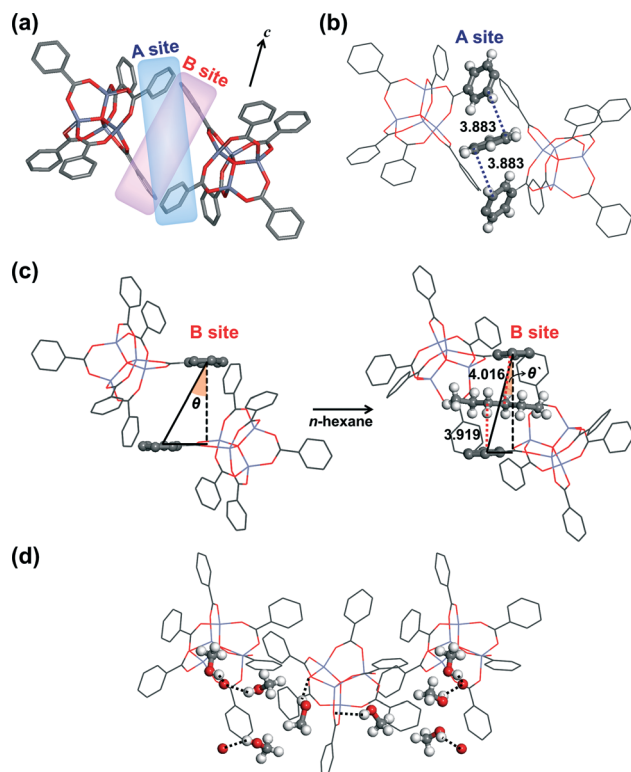


**Fig. 2** Host-guest and guest-guest interactions in (a) **1**, (b) **1**<sub>benzene</sub>, (c) **1**<sub>hexane</sub>, and (d) **1**<sub>MeOH</sub>. In (c),  $\theta$  and  $\theta'$  are the offset angles of the two phenyl rings. Colour scheme: C (grey), O (red), H (white), and Zn (purple).

between the parallel phenyl rings in the B sites provided the hexane molecules with the appropriate environment for effective CH- $\pi$  interactions with both phenyl rings. Moreover, the offset angle of two phenyl rings changed from 29.30° ( $\theta$ ) to 20.02° ( $\theta'$ ), and the distance between the two phenyl rings became longer from 7.668 to 8.062 Å, which provides enough space to accommodate hexane molecules and generates CH- $\pi$  interactions more efficiently (Fig. 2c). This offset angle

change is closely related to the cell parameter changes. However, in **1**<sub>MeOH</sub>, there were no significant interactions between the MeOH molecules and the host framework except for a hydrogen bond of one methanol molecule with a carboxylate oxygen atom (Fig. 2d). Instead, the included methanol molecules participated in the guest-guest interactions with water molecules *via* hydrogen bonding, thus forming stronger host-host interactions *via*  $\pi$ - $\pi$  interactions between the phenyl rings (Fig. S10†). The TGA data for the guest-exchanged compounds also reflected the strength of the host-guest interaction depending on the guest molecules. The temperature at which the host lost its guest molecules was shifted from their boiling point depending on the strength of the host-guest interactions (Fig. S11† and Table 1); in **1**<sub>benzene</sub>, the included benzene molecules were liberated at 100 °C while the boiling point of neat benzene is 80.1 °C. **1**<sub>hexane</sub> showed a much larger difference between those temperatures, 170 vs. 68.5 °C. In contrast, methanol molecules in **1**<sub>MeOH</sub> evaporated completely at 60 °C, near the boiling point of MeOH, indicating its weak host-guest interactions.

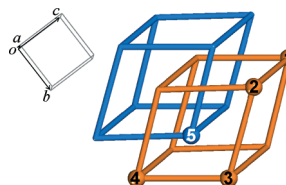
After guest exchange, the space groups remained as *R32* for **1**<sub>benzene</sub> and changed to *R3c* for **1**<sub>hexane</sub> and **1**<sub>MeOH</sub>, and the dimensions of the unit cells changed significantly (Table 1 and S1-4†). This was primarily due to interframework sliding, which was triggered by the newly formed host-guest, host-host, or guest-guest interactions upon guest exchange, as described previously. The cell volume of **1** slightly increased from 21 331(6) to 21 540(6) Å<sup>3</sup> for **1**<sub>benzene</sub>, and significantly decreased to 19 605(6) and 19 202(5) Å<sup>3</sup> for **1**<sub>hexane</sub> and **1**<sub>MeOH</sub>, respectively. Specially, the guest molecule exchange from DMF to MeOH led to the greatest changes in the cell parameters, which corresponded to a reduction of the cell volume by 10%, accompanied by a decrease in the void volume by 23.9%. The changes in the cell parameters were attributed to the compression of the individual pcu nets and the sliding motion between the interframework along the *c* axis as shown in the figure under Table 1. Since each edge of the pcu net conformed to the flexible CPMA ligand linking the

**Table 1** Selected crystal parameters for **1**, **1**<sub>benzene</sub>, **1**<sub>hexane</sub> and **1**<sub>MeOH</sub>

	<i>a</i> = <i>b</i> (Å)	<i>c</i> (Å)	Cell volume (Å <sup>3</sup> )	Void volume <sup>a</sup> (Å <sup>3</sup> )	Intraframework O...O distance <sup>b</sup> (Å <sup>3</sup> )			Interframework O...O distance <sup>b</sup> (Å <sup>3</sup> )		Desolvation temperature <sup>c</sup> (°C)	Boiling point (°C)
					①-②	②-③	①-④	④-⑤	①-⑤		
<b>1</b> (DMF)	18.985(3)	68.340(14)	21 331(6)	10 333.5 (48.4%)	15.539	16.080	33.794	12.104	21.690	150	152
<b>1</b> <sub>benzene</sub>	19.168(3)	67.695(13)	21 540(6)	10 814.4 (50.2%)	15.582	16.029	33.535	12.519	21.016	100	80.1
<b>1</b> <sub>hexane</sub>	18.653(3)	65.066(13)	19 605(6)	8301.0 (42.3%)	15.283	15.283	32.533	11.000	21.533	170	68.5
<b>1</b> <sub>MeOH</sub>	18.118(3)	67.542(14)	19 202(5)	7865.3 (41.0%)	15.367	15.367	33.771	11.119	22.652	60	64.7

<sup>a</sup> Calculated by PLATON. <sup>b</sup> The numbering was indicated in the figure in the right.

<sup>c</sup> The desolvation temperature of guest molecules from MOF **1** was determined by TGA.



oxo clusters (Fig. 1b), new interactions altered the degree of framework compression, which can be expressed by the distances between the oxo centres in the intraframework (Table 1). Consequently, since the oxo centres in positions O1 and O4 were located along the *c* axis, this framework compression directly changed the length of the *c* parameter. In addition, the sliding motion led to effective host–guest or host–host interactions, as described previously, and changed the interframework O...O distances between O4 and O5 as well O1 and O5. Accordingly, **1**<sub>hexane</sub> and **1**<sub>MeOH</sub> underwent intraframework compression as well as the sliding motion, while in **1**<sub>benzene</sub>, these movements did not occur significantly because the benzene molecules fit into the A sites and did not require significant structural changes. On the other hand, the offset change in **1**<sub>hexane</sub> led to a higher degree of *c* axis compression than those in the other compounds, due to the CH– $\pi$  interactions between hexane and the phenyl rings on the *c* axis (Fig. S12<sup>†</sup>). In **1**<sub>MeOH</sub>, the major changes were the reduction of *a* and *b* parameters, which was due to strong host–host interactions. The peak positions of the measured XRPD patterns for **1** and the guest-exchanged products coincided with those of the simulated patterns derived from the X-ray single-crystal data, except that the XRPD pattern of **1**<sub>MeOH</sub> was somewhat different from the simulated pattern (Fig. S13<sup>†</sup>). This may be because **1**<sub>MeOH</sub> rapidly lost MeOH molecules during the measurements. The compression of the lattice plane of **1**<sub>hexane</sub> and **1**<sub>MeOH</sub> was confirmed by the shift of the XRPD peaks to the higher angle region compared to those of **1** or **1**<sub>benzene</sub> (Fig. S13<sup>†</sup>).

## Conclusions

A Zn<sub>4</sub>O-containing doubly interpenetrated MOF with a *pcu* net, [Zn<sub>4</sub>O(CPMA)<sub>3</sub>] $\cdot$ 6DMF (**1**) underwent single-crystal to single-crystal transformations upon guest exchange of DMF molecules with benzene, *n*-hexane, and methanol. SCD analysis revealed that the structural transformations involving the sliding motions of the interpenetrated networks as well as the dynamic movements of the molecular components were triggered by the host–guest interactions. The  $\pi$ – $\pi$  interactions in **1**<sub>benzene</sub> and CH– $\pi$  interactions in **1**<sub>hexane</sub> between the introduced solvent molecules and the phenyl rings of the CPMA<sup>2-</sup> ligand in the host framework were discussed with respect to the resulting structures. Interestingly, **1** showed a significant decrease in cell volume from 21 331 to 19 202 Å<sup>3</sup> (10%) upon guest exchange with methanol, which indicated that in **1**<sub>MeOH</sub>, the dominant force which determined the structure was the interframework interactions rather than the host–guest interactions. In order to facilitate potential applications of MOFs in molecular sensing, separation, catalysis, and storage, it is essential to understand how MOFs respond to external stimuli and determine the host–host, host–guest, and guest–guest interactions involved in the responses *via* X-ray single-crystal structural analysis.

## Acknowledgements

This work was supported by the Basic Science Research Program through the National Research Foundation of Korea (NRF) funded by the Ministry of Education, Science and Technology (NRF-2005-0093842 and NRF-2013R1A1A3010846), and the Korea CCS R&D Centre (KCRC) grant funded by the Korean government (Ministry of Science, ICT & Future Planning) (NRF-2014M1A8A1049255). J. H. L. acknowledges a Global PhD Fellowship (NRF-2013H1A2A1033501).

## Notes and references

- (a) J. Park, D. Feng, S. Yuan and H.-C. Zhou, *Angew. Chem., Int. Ed.*, 2015, **54**, 430; (b) I.-H. Park, A. Chanthapally, Z. Zhang, S. S. Lee, M. J. Zaworotko and J. J. Vittal, *Angew. Chem.*, 2014, **126**, 424; (c) S. Henke, A. Schneemann, A. Wütscher and R. A. Fischer, *J. Am. Chem. Soc.*, 2012, **134**, 9464; (d) K. L. Mulfort and J. T. Hupp, *J. Am. Chem. Soc.*, 2007, **129**, 9604; (e) E. Y. Lee, S. Y. Jang and M. P. Suh, *J. Am. Chem. Soc.*, 2005, **127**, 6374.
- (a) E. D. Bloch, L. J. Murray, W. L. Queen, S. Chavan, S. N. Maximoff, J. P. Bigi, R. Krishna, V. K. Peterson, F. Grandjean, G. J. Long, B. Smit, S. Bordiga, C. M. Brown and J. R. Long, *J. Am. Chem. Soc.*, 2011, **133**, 14814; (b) M.-H. Zeng, Q.-X. Wang, Y.-X. Tan, S. Hu, H.-X. Zhao, L.-S. Long and M. Kurmoo, *J. Am. Chem. Soc.*, 2010, **132**, 2561; (c) X.-N. Cheng, W.-X. Zhang and X.-M. Chen, *J. Am. Chem. Soc.*, 2007, **129**, 15738; (d) G. J. Halder, C. J. Kepert, B. Moubaraki, K. S. Murry and J. D. Cashion, *Science*, 2002, **298**, 1762.
- (a) K. Biradha, Y. Hongo and M. Fujita, *Angew. Chem., Int. Ed.*, 2002, **41**, 3395; (b) M. P. Suh, J. W. Ko and H. J. Choi, *J. Am. Chem. Soc.*, 2002, **124**, 10976.
- (a) J.-P. Zhang, P.-Q. Liao, H.-L. Zhou, R.-B. Lin and X.-M. Chen, *Chem. Soc. Rev.*, 2014, **43**, 5789; (b) S. Neogi, S. Sen and P. K. Bharadwaj, *CrystEngComm*, 2013, **15**, 9239; (c) S. Horike, S. Shimomura and S. Kitagawa, *Nat. Chem.*, 2009, **1**, 695; (d) M. P. Suh and Y. E. Cheon, *Aust. J. Chem.*, 2006, **59**, 605.
- (a) M. P. Suh, H. R. Moon, E. Y. Lee and S. Y. Jang, *J. Am. Chem. Soc.*, 2006, **128**, 4710; (b) E. Y. Lee and M. P. Suh, *Angew. Chem., Int. Ed.*, 2004, **43**, 2798.
- (a) H. J. Park and M. P. Suh, *Chem. – Eur. J.*, 2008, **14**, 8812; (b) C.-D. Wu and W. Lin, *Angew. Chem., Int. Ed.*, 2005, **44**, 1958.
- (a) H. J. Park, D.-W. Lim, W. S. Yang, T.-R. Oh and M. P. Suh, *Chem. – Eur. J.*, 2011, **17**, 7251; (b) J. Y. Lee, S. Y. Lee, W. Sim, K.-M. Park, J. Kim and S. S. Lee, *J. Am. Chem. Soc.*, 2008, **130**, 6902; (c) J.-P. Zhang, Y.-Y. Lin, W.-X. Zhang and X.-M. Chen, *J. Am. Chem. Soc.*, 2005, **127**, 14162.
- H. J. Park, Y. E. Cheon and M. P. Suh, *Chem. – Eur. J.*, 2010, **16**, 11662.

- 9 H. J. Choi and M. P. Suh, *J. Am. Chem. Soc.*, 2004, **126**, 15844.
- 10 D.-W. Lim, S. A. Chyun and M. P. Suh, *Angew. Chem., Int. Ed.*, 2014, **53**, 7819.
- 11 (a) B. F. Abrahams, H. E. Maynard-Casely, R. Robson and K. F. White, *CrystEngComm*, 2013, **15**, 9729; (b) A. Husain, M. Ellwart, S. A. Bourne, L. Öhrström and C. L. Oliver, *Cryst. Growth Des.*, 2013, **13**, 1526; (c) H.-L. Jiang, T. A. Makal and H.-C. Zhou, *Coord. Chem. Rev.*, 2013, **257**, 2232; (d) R. Yang, L. Li, Y. Xiong, J.-R. Li, H.-C. Zhou and C.-Y. Su, *Chem. – Asian J.*, 2010, **5**, 2358.
- 12 T. K. Maji, R. Masuda and S. Kitagawa, *Nat. Mater.*, 2007, **6**, 142.
- 13 Y. Takashima, V. M. Martínez, S. Furukawa, M. Kondo, S. Shimomura, H. Uehara, M. Nakahama, K. Sugimoto and S. Kitagawa, *Nat. Commun.*, 2011, **2**, 168.
- 14 H. Aggarwal, P. M. Bhatt, C. X. Bezuidenhout and L. J. Barbour, *J. Am. Chem. Soc.*, 2014, **136**, 3776.
- 15 T. K. Kim, J. H. Lee, D. Moon and H. R. Moon, *Inorg. Chem.*, 2013, **52**, 589.
- 16 PLATON program: A. L. Spek, *Acta Crystallogr., Sect. C: Struct. Chem.*, 2015, **71**, 9.
- 17 (a) M. L. Waters, *Curr. Opin. Chem. Biol.*, 2002, **6**, 736; (b) J. Singh and J. M. Thornton, *J. Mol. Biol.*, 1991, **218**, 837; (c) C. A. Hunter and J. K. M. Sanders, *J. Am. Chem. Soc.*, 1990, **112**, 5525.